

Electrical Bistability around Room Temperature in an Unprecedented One-Dimensional Coordination Magnetic Polymer

Pilar Amo-Ochoa,[†] Esther Delgado,^{*,†} Carlos J. Gómez-García,[‡] Diego Hernández,[†] Elisa Hernández,[†] Avelino Martín,[§] and Félix Zamora^{*,†}

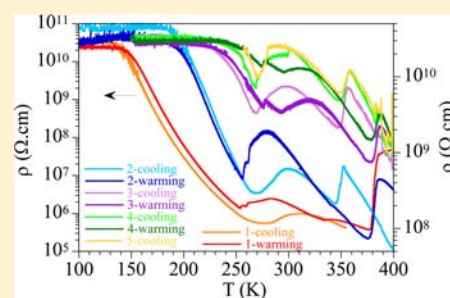
[†]Departamento de Química Inorgánica, Universidad Autónoma de Madrid, 28049 Madrid, Spain

[‡]Instituto de Ciencia Molecular, Universidad de Valencia, C/Catedrático José Beltrán, 2, 46980 Paterna, Valencia, Spain

[§]Departamento de Química Inorgánica, Universidad de Alcalá de Henares, Campus Universitario, E-28871, Alcalá de Henares, Spain

Supporting Information

ABSTRACT: The synthesis, crystal structure, and physical properties of an unprecedented one-dimensional (1D) coordination polymer containing $[\text{Fe}_2(\text{S}_2\text{C}_6\text{H}_2\text{Cl}_2)_4]^{2-}$ entities bridged by dicationic $[\text{K}_2(\mu\text{-H}_2\text{O})_2(\text{THF})_4]^{2+}$ units are described. The magnetic properties show that the title compound presents pairwise Fe–Fe antiferromagnetic interactions that can be well reproduced with a $S = 1/2$ dimer model with an exchange coupling, $J = -23 \text{ cm}^{-1}$. The electrical conductivity measurements show that the title compound is a semiconductor with an activation energy of about 290 meV and two different transitions, both with large hysteresis of about 60 and 30 K at 260–320 K and 350–380 K, respectively. These two transitions are assumed to be due to slight structural changes in the cation–anion interactions. Differential Scanning Calorimetry confirms the presence of both transitions. This compound represents the first sample of a coordination polymer showing electrical bistability.



INTRODUCTION

Since a long time ago, 1,2-dithiolene transition metal complexes are a subject of high research interest as a consequence of their rich redox chemistry, versatility in their coordination modes, and biological function, as well as for their well-known magnetic and electrical conducting properties.^{1–8}

Despite the fact that square-planar or tetrahedral mononuclear metal bis(dithiolato) compounds are common for Ni, Co, Pd, Pt, Cu, and Au metal ions,^{5,9–13} examples of $[\text{Fe}(\text{dithiolato})_2]^{z-}$ ($z = 1$ or 2) derivatives with these types of geometries are scarce because of their strong tendency to dimerize yielding the stable square-pyramidal $[\text{Fe}_2(\text{dithiolato})_4]^{z-}$ entity ($z = 0, 1,$ or 2).¹⁴ Additionally, it has been reported that the presence of extra-donor atoms such as nitrogen in the dithiolato ligands of the transition metal bis(dithiolato) anions, able to coordinate to metal cations, favors the formation of structures of different dimensionality, including one-dimensional (1D) chains.¹⁵

On the other hand, carbonyl substitution reactions by strong donating ligands, mainly phosphines or CN^- , in diiron hexacarbonyl-bis(thiolato) or -dithiolato compounds are well-documented. Studies on these types of compounds have spread because they can be considered as structurally related to the active site of the $[\text{FeFe}]$ -hydrogenases.^{16–23}

A different reactivity has been observed in these iron derivatives depending on the incoming ligands, as well as on the nature of the dithiolato. Thus, a simple substitution of CO by CN^- is observed in compound $[\text{Fe}_2(\text{S}_2\text{C}_3\text{H}_6)(\text{CO})_6]^{19}$ to yield $[\text{Fe}_2(\text{S}_2\text{C}_3\text{H}_6)(\text{CO})_4(\text{CN})_2]^{2-}$, while formation of $[\text{Fe}$

$(\text{S}_2\text{C}_6\text{H}_4)(\text{CO})_2(\text{CN})_2]^{2-}$ takes place using $[\text{Fe}_2(\text{S}_2\text{C}_6\text{H}_4)(\text{CO})_6]$ as precursor instead.²⁴ In the latter reaction $[\text{Fe}_2(\text{S}_2\text{C}_6\text{H}_4)(\text{CO})_6]$ undergoes a disproportionative transformation to afford Fe^0 and the 16 electrons unstable $\text{Fe}(\text{II})$ specie $[\text{Fe}(\text{S}_2\text{C}_6\text{H}_4)(\text{CO})_2(\text{CN})]^-$, that subsequently dimerizes to form the more stable compound $[\text{Fe}(\text{S}_2\text{C}_6\text{H}_4)(\text{CO})_2(\text{CN})_2]^{2-}$.²⁵ It is also known that the reaction between $[\text{PPN}][\text{Fe}(\text{S}_2\text{NH}-\text{C}_6\text{H}_4)(\text{CO})_2(\text{CN})]$ and 1,2-benzenedithiol affords the iron bis(dithiolato) derivative $[\text{PPN}][\text{Fe}(\text{S}_2\text{C}_6\text{H}_4)_2(\text{THF})]$ (PPN = bis(triphenylphosphine)-iminium).²⁶

Coordination polymers have deserved increasing attention mainly because of their structural variety, multifunctional properties, and potential applications from both material science and crystal engineering points of view;^{27,28} however, to the best of our knowledge examples of 1D iron bis(dithiolato) coordination polymers are unknown.

Taking into account the above-mentioned, in this study we have focused on exploring the role of the 3,6-dichlorobenzene-1,2-dithiolato ligand, which contains chloride as additional donor atom, and the behavior of the K^+ cation to form an iron bis(dithiolato) polymer, in the reaction of $[\text{Fe}_2(\text{S}_2\text{C}_6\text{H}_2\text{Cl}_2)(\text{CO})_6]$ with an excess of the dithiolene, $\text{H}_2\text{S}_2\text{C}_6\text{H}_2\text{Cl}_2$, in presence of K_2CO_3 . Here we report the synthesis, characterization, and physical properties of an unprecedented 1D coordination polymer based on $[\text{Fe}_2(\text{S}_2\text{C}_6\text{H}_2\text{Cl}_2)_4]^{2-}$ entities.

Received: January 21, 2013

Published: May 1, 2013

EXPERIMENTAL SECTION

Materials and Methods. All reactions were carried out under argon atmosphere. Solvents were dried using standard methods.²⁹ IR spectra were recorded on a Perkin-Elmer Spectrum BX FT-IR spectrophotometer. Mass spectrometric measurements recorded in ESI⁻ and ESI⁺ mode were obtained on a Electrospray (ESI) QSTAR hybrid quadrupole Time-of-Flight (Q-TOF) (Applied Biosystems). Elemental analyses were performed on an Elemental Analyzer LECO CHNS-932. $[\text{Fe}_2(\text{S}_2\text{C}_6\text{H}_2\text{Cl}_2)(\text{CO})_6]$ was prepared according to published procedures.¹⁶ $\text{H}_2\text{S}_2\text{C}_6\text{H}_2\text{Cl}_2$ and K_2CO_3 were obtained commercially from Sigma-Aldrich.

Direct current (DC) electrical conductivity measurements were carried out with the four or two contacts methods (depending on the size of the crystals) on ten single crystals of compound **1** in the temperature range 400–2 K. The contacts were made with Pt wires (25 μm diameter) using graphite paste. The samples were measured in a Quantum Design PPMS-9 equipment connected to an external voltage source (Keithley model 2400 source-meter) and amperometer (Keithley model 6514 electrometer). The samples were measured by applying a constant voltage of 10 or 20 V and measuring the intensity. All the conductivity quoted values have been measured in the voltage range where the crystals are Ohmic conductors. The cooling and warming rates were 1 K/min. Since the first crystal measured showed that in the temperature range 2–150 K the resistance of the sample exceeded our detection limit ($5 \times 10^{11} \Omega$), we only cooled the other crystals down to 100 K. A typical measurement consists in a first cooling scan from 300 to 100 K followed by a warming scan from 100 to 400 K. The consecutive cycles (up to four) were done from 400 to 100 K and from 100 to 400 K, always with the same cooling and warming rates.

Variable temperature susceptibility measurements were carried out in the temperature range 2–300 K with an applied magnetic field of 0.1 T on a polycrystalline sample of compound **1** (with a mass of 59.95 mg) with a Quantum Design MPMS-XL-5 SQUID magnetometer. The isothermal magnetization was made on the same sample at 2 K with magnetic fields of up to 5 T. The susceptibility data were corrected for the sample holder previously measured using the same conditions and for the diamagnetic contributions of the salt as deduced by using Pascal's constant tables ($\chi_{\text{dia}} = -363.56 \times 10^{-6} \text{ emu mol}^{-1}$).³⁰

Differential Scanning Calorimetry (DSC) measurements were performed in the temperature range 400–200 K on a polycrystalline sample of compound **1** on a Mettler Toledo DSC-821e. The temperature was scanned from 300 to 200 K in a first cooling scan, followed by a first heating scan from 200 to 400 K, a second cooling scan from 400 to 200 K, a second heating scan from 200 to 400 K, and a third cooling scan from 400 to 300 K. All the scans were performed with a temperature scanning rate of 2 K/min.

X-ray Structure Analysis of 1. Crystals of complex **1** were grown from THF/ H_2O /*n*-Hexane. Then crystals were removed from the Schlenk flask and covered with a layer of a viscous perfluoropolyether (FomblinY). A suitable crystal was selected with the aid of a microscope, attached to a glass fiber, and immediately placed in the low temperature nitrogen stream of the diffractometer. The intensity data sets were collected at 200 K on a Bruker-Nonius Kappa CCD diffractometer equipped with an Oxford Cryostream 700 unit. The structure was solved, using the WINGX package³¹ by direct methods (SHELXS-97) and refined by least-squares against F^2 (SHELXL-97).³² All non-hydrogen atoms were anisotropically refined. The hydrogen atoms were positioned geometrically and refined by using a riding model (Table 1).

Synthesis of Compound $[\text{K}_2(\mu\text{-H}_2\text{O})_2(\text{THF})_4]_n[\text{Fe}_2(\text{S}_2\text{C}_6\text{H}_2\text{Cl}_2)_4]_n$ 1. To a solution of K_2CO_3 (120 mg, 0.86 mmol) in 15 mL of dimethylformamide (DMF) previously degassed $[\text{Fe}_2(\text{S}_2\text{C}_6\text{H}_2\text{Cl}_2)(\text{CO})_6]$ (300 mg, 0.61 mmol) and $\text{H}_2\text{S}_2\text{C}_6\text{H}_2\text{Cl}_2$ (386 mg, 1.83 mmol) were added. The mixture was stirred at room temperature for 8 h and then the solvent was removed until dryness. The residue was washed several times with dichloromethane, and suitable crystals for X-ray analysis of compound **1** were obtained from a solution of tetrahydrofuran (THF) with a few drops of DMF, followed by

Table 1. Crystal Data and Structure Refinement for **1**

1	
moiety formula	$\text{C}_{20}\text{H}_{22}\text{Cl}_4\text{FeK}_4\text{O}_3\text{S}_4$
formula weight	675.37
temperature [K]	200(2)
wavelength (MoK α) [Å]	0.71073
crystal system	monoclinic
space group	$P2_1/c$
<i>a</i> [Å]	9.361(1)
<i>b</i> [Å]	22.276(5)
<i>c</i> [Å]	13.218(3)
β (deg)	103.525(11)
μ (mm ⁻¹)	1.451
<i>F</i> (000)	1372
crystal size [mm ³]	0.35 × 0.2 × 0.18
θ range	3.03 to 27.53°
index ranges	−12 to 11, −28 to 28, 0 to 17
collected reflections	43336
independent reflections	6142
goodness-of-fit on F^2	0.97
final <i>R</i> indices [$F > 4\sigma(F)$]	<i>R</i> 1 = 0.045, <i>wR</i> 2 = 0.093
<i>R</i> indices (all data)	<i>R</i> 1 = 0.120, <i>wR</i> 2 = 0.111
largest diff. peak/hole [$e \text{ Å}^{-3}$]	0.656/−0.438

addition of H_2O and *n*-hexane at room temperature. Yield: 246 mg, 30% (Found: C, 27.83; H, 1.66; S, 23.52. Calc. for $\text{C}_{24}\text{H}_8\text{Cl}_8\text{Fe}_2\text{K}_2\text{S}_8\cdot 2\text{H}_2\text{O}$: C, 27.12; H, 1.13; S, 24.10%). Electrospray mass spectrum (MeOH, *m/z*) in negative-ion mode: 473.7 $[\text{Fe}(\text{S}_2\text{C}_6\text{H}_2\text{Cl}_2)_2]^-$, in positive-ion mode: 39 $[\text{K}]^+$.

RESULTS AND DISCUSSION

Synthesis and Structural Characterization. A mixture of the precursor complex $[\text{Fe}_2(\text{S}_2\text{C}_6\text{H}_2\text{Cl}_2)(\text{CO})_6]$, the ligand $\text{H}_2\text{S}_2\text{C}_6\text{H}_2\text{Cl}_2$, and K_2CO_3 in DMF was stirred for 8 h at room temperature. The IR spectrum of the resulting solution indicated a complete release of the CO ligands with the disappearance of their characteristic IR features. After complete removal of the solvent, compound **1** was recrystallized in THF/ $\text{DMF}/\text{H}_2\text{O}/n$ -hexane (Scheme 1) yielding crystals suitable for single X-ray diffraction studies.

The crystal structure of compound $[\text{K}_2(\mu\text{-H}_2\text{O})_2(\text{THF})_4]_n[\text{Fe}_2(\text{S}_2\text{C}_6\text{H}_2\text{Cl}_2)_4]_n$ **1** reveals the formation of a monodimensional polymer containing dianionic $[\text{Fe}_2(\text{S}_2\text{C}_6\text{H}_2\text{Cl}_2)_4]^{2-}$ entities linked by heptacoordinated potassium complexes (Figure 1).

As mentioned before, it is known that transition metal bis(dithiolato) compounds containing extra-donating atoms in the dithiolato ligands, in addition to the sulfur ones, may form anion–cation 1D chains. Thus, several examples have been reported in which N-donor atoms of anionic metal bis(dithiolato) entities are coordinated to the metal of the counter-cations yielding monodimensional coordination polymers. Some examples are as follows: $[\text{Na}(\text{N}_{15}\text{C}_5)]_2[\text{Pt}(i\text{-mnt})_2]$ ($\text{N}_{15}\text{C}_5 = 2,3$ -naphto-15-crown-5; *i*-mnt = *cis*-1,1-dicyanoethylene-2,2-dithiolato),³³ $[\text{K}(\text{DC18C6-A})]_2[\text{M}(\text{mnt})_2]$ (DC18C6-A = *cis-syn-cis*-dicyclohexyl-18-crown-6, isomer A; M = Ni, Pd, Pt; mnt = 1,2-dicyanoethene-1,2-dithiolato = maleonitriledithiolato = $[\text{C}_2\text{S}_2(\text{CN})_2]^{2-}$)³⁴ and $[\text{Ni}(\text{cyclam})]_2[\text{Cu}(\text{tfadt})_2]$ (cyclam = 1,4,8,11-tetraazacyclotetradecane; tfadt = 3-(trifluoromethyl)acrylonitrile-2,3-dithiolato).³⁵ However, to the best of our knowledge, compound **1** represents the

Scheme 1. Reaction Leading to Formation of Compound 1

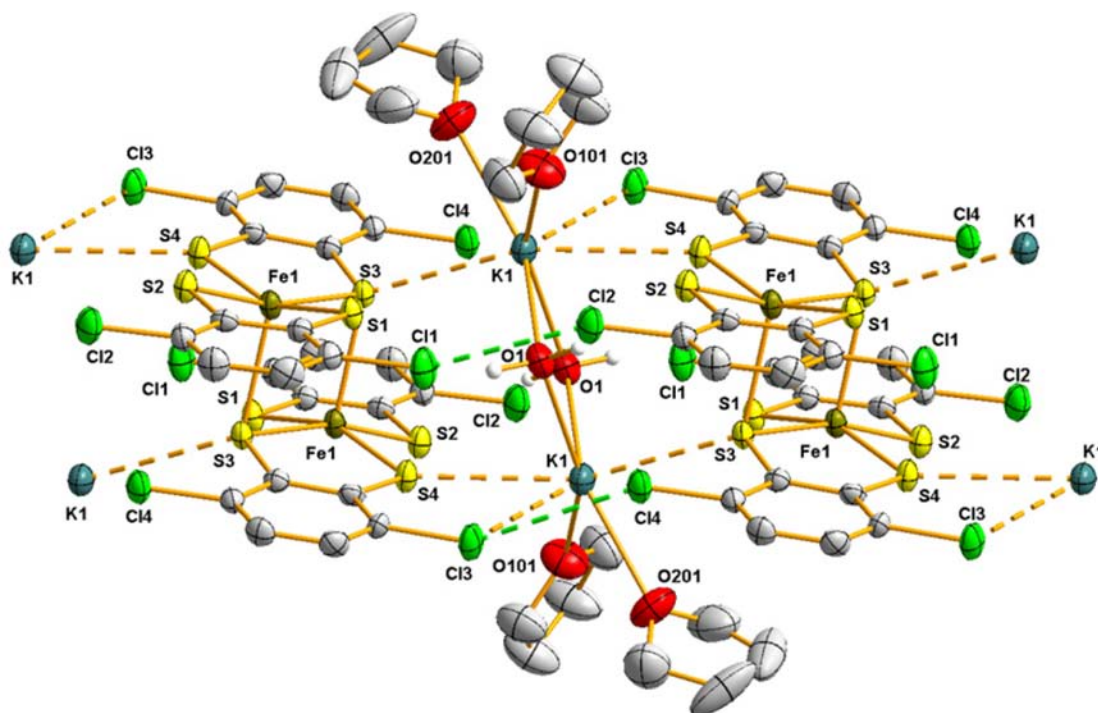
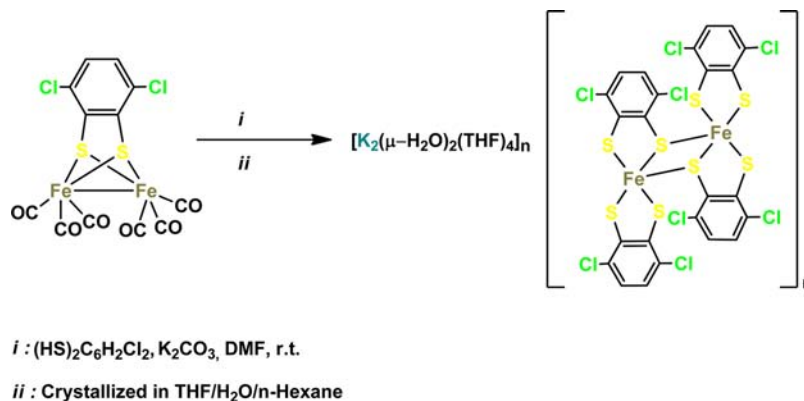


Figure 1. ORTEP drawing of compound 1. Thermal ellipsoids at 50% probability level.

first example of a 1D coordination polymer containing iron dithiolato entities.

The X-ray analyses of the crystal structure of **1** reveal that the dianionic unit $[\text{Fe}_2(\text{S}_2\text{C}_6\text{H}_2\text{Cl}_2)_4]^{2-}$ forms a centrosymmetric dimer in which each iron atom shows the expected 4 + 1 square base pyramidal geometry. This is a typical coordination geometry found in many iron(III) bis(dithiolato) compounds, and is a consequence of the strong tendency for dimerization of the monoanionic $[\text{Fe}(\text{dithiolato})_2]^-$ species. Selected distances and angles are given in Table 2. The basal Fe–S bond distances [Fe–S1 = 2.224(1), Fe–S2 = 2.217(1), Fe–S3 = 2.229(1), and Fe–S4 = 2.223(1) Å] are shorter than the axial one [2.488(1) Å], and they are all similar to those found in other dimeric bis(dithiolato) derivatives such as α - $[\text{FeCp}^*_2][\text{Fe}(\text{mnt})_2](\text{CH}_3\text{CN})_2$ (mnt = maleonitriledithiolato),³⁶ $[\text{n-Bu}_4\text{N}]_2[\text{Fe}(\text{cbdt})_2]_2$ (cbdt = 4-cyanobenzene-1,2-dithiolato),³⁷ $[\text{n-Bu}_4\text{N}]_2[\text{Fe}(\text{dcbdt})_2]_2$ (dcbdt = 4,5-dicyanobenzene-1,2-dithiolato),³⁸ $[\text{Ph}_4\text{As}]_2[\text{Fe}(\text{qdt})_2]_2$ (qdt = quinoxalinedithiolato),³⁹ and $[\text{Et}_3\text{NH}]_2[\text{Fe}(\text{pdt})_2]_2$ (pdt = pyrazine-2,3-dithiolo-

Table 2. Selected Bond Lengths (Å) and Angles (deg) for Complex 1

Fe1–S1	2.224(1)	K1–S3	3.272(1)
Fe1–S2	2.217(1)	K1–S4	3.258(1)
Fe1–S3	2.229(1)	K1–Cl3	3.334(1)
Fe1–S4	2.223(1)	K1–O1	2.779(3)
Fe1–S3	2.488(1)	K1–O1	2.796(3)
Fe1–Fe1	3.102(1)	K1–O101	2.674(3)
		K1–O201	2.734(3)
Fe1–S3–Fe1	82.04(3)	O101–K1–O201	73.6(1)
S2–Fe1–S4	89.06(4)	O101–K1–O201	73.6(1)
S2–Fe1–S1	88.57(4)	S4–K1–S3	158.70(4)
S4–Fe1–S3	89.14(4)	S4–K1–Cl3	58.22(3)
S1–Fe1–S3	87.52(4)	S3–K1–Cl3	113.45(4)

to).⁴⁰ Moreover, the iron atoms are shifted out of the least-squares plane defined by the four sulfur atoms by 0.357 Å. The presence of two Cl⋯Cl weak interactions between two

$[\text{Fe}_2(\text{S}_2\text{C}_6\text{H}_2\text{Cl}_2)_4]^{2-}$ units (Figure 1) is also noticeable as confirmed by the $\text{Cl1}\cdots\text{Cl2} = 3.401(2)$ Å and $\text{Cl3}\cdots\text{Cl4} = 3.461(2)$ Å lengths, in the range of the sum of the van der Waals radii,⁴¹ together with the averaged angles $\text{C}-\text{Cl}\cdots\text{Cl}$ of $151.7(6)^\circ$ and $149.2(1)^\circ$, respectively. These data let us to classify these interactions as type I, according to Nyburg⁴² and Fourmigué.^{43,44} The most remarkable feature of this structure is the presence of potassium complexes, formulated as $[\text{K}_2(\mu\text{-H}_2\text{O})_2(\text{THF})_4]^{2+}$, acting as counter-cations and bridging the anionic $[\text{Fe}_2(\text{S}_2\text{C}_6\text{H}_2\text{Cl}_2)_4]^{2-}$ entities giving rise to a linear coordination polymer running along the *a* direction (Figure 2).

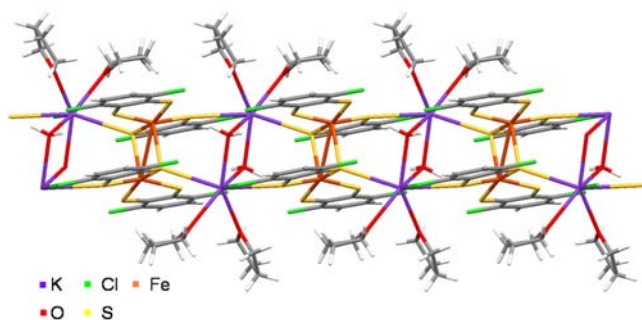


Figure 2. View of a polymer chain of **1** along the *a* axis.

In the cations, each K^+ is coordinated to two terminal THFs and two bridging H_2O ligands. Both molecules coordinate the K^+ during the crystallization process. To complete the heptacoordination sphere each potassium atom is bonded to one sulfur and one chloride atoms of one neighboring dianionic unit, forming a five-member chelate ring, and to a sulfur atom of the another neighboring dianionic entity.

High co-ordination numbers in potassium complexes are known, but most of them showing oxygen donor atoms, particularly from water molecules. The $\text{K}-\text{O}$ bond distances for the bridging water ligands in compound **1** [$2.779(3)$ and $2.796(3)$ Å] fit well with other potassium complexes containing water as ligand. Thus, analogous $\text{K}-\text{O}$ bond distances are found in other heptacoordinated potassium complexes such as $[\text{K}][\text{C}_7\text{H}_7\text{BrNO}_2\text{S}]\cdot\text{H}_2\text{O}$,⁴⁵ $[\text{K}][\text{C}_6\text{H}_4\text{Cl}_2\text{NO}_2\text{S}]\cdot\text{H}_2\text{O}$,⁴⁶ and $[\text{K}(\text{calix}[8]\text{arene-H})(\text{THF})_4(\text{H}_2\text{O})_7]$.⁴⁷ Moreover, the latter shows a $\text{K}-\text{O}(\text{THF})$ bond distance close to those observed in compound **1** [$2.674(3)$ and $2.734(3)$ Å]. Additionally, the $\text{K}-\text{S}$ bond distances in **1** [$3.272(1)$ and $3.258(1)$ Å] compare well with those described for $[\text{K}(18\text{-crown-6})(\text{SCPh}_3)(\text{G})_{0.5}]$ ($\text{G} = \text{C}_6\text{H}_6$ or THF).⁴⁸ Finally, the $\text{K}-\text{Cl}$ bond distance of $3.334(1)$ Å is within the range ($3.232\text{--}3.674$ Å, average value = 3.424 Å) found in the nine reported compounds with $\text{K}-\text{Cl}$ bonds between Cl -substituted aromatic rings and K^+ cations.^{49–56}

As far as we know, compound **1** represents the first example of a 1D coordination polymer showing iron dithiolato derivatives as building blocks. Furthermore, among the structures reported to date containing $[\text{Fe}(\text{dithiolato})_2]$ complexes, compound **1** is the first example containing alkali metals (K^+ in this case) as counterions. These two unique characteristics of compound **1** (1D polymeric structure and the presence of K^+ cations) seem to be closely related. This idea is supported by a detailed analysis of all the reported crystal structures containing $[\text{Fe}(\text{dithiolato})_2]$ units (either neutral or anionic). Thus, a search in the CCDC database⁵⁷ shows a total of 54 different compounds: 48 with dimeric $[\text{Fe}(\text{dithiolato})_2]_2$ units and only 6 with monomeric $[\text{Fe}(\text{dithiolato})_2]$ entities.

Among the 48 dimerized compounds, in 41 cases the Fe atoms present a square pyramidal geometry (as in **1**) whereas in the remaining 7 examples the coordination number is six. On the other hand, among the six monomeric $[\text{Fe}(\text{dithiolato})_2]$ complexes, five show a square planar geometry and one presents a tetrahedral one. In all the structures where the $[\text{Fe}(\text{dithiolato})_2]$ units are anionic (45 of 54) the cations are very big and have no coordinating capacity, precluding the formation of a polymeric structure. These noncoordinating cations are tetra-alkyl-ammonium derivatives, NR_4^+ (20 cases), AsPh_4^+ (6 cases), metallocenium (MCp_2 and $\text{MCp}^*_{2,2}$, 6 cases), pyridinium derivatives (8 cases), tetrathiafulvalene-type donors (3 cases) and PPh_4^+ (2 cases). Therefore, it seems that the presence in **1** of a metallic counterion that can be coordinated by the donor atoms of the dianionic entities is the origin of the formation of this unprecedented polymeric structure in **1**.

Magnetic Measurements. Magnetic susceptibility measurements carried out in compound **1** in the temperature range 2–300 K show a continuous decrease of the $\chi_m T$ value from about $1.8 \text{ cm}^3 \text{ K mol}^{-1}$ at room temperature to about $0.18 \text{ cm}^3 \text{ K mol}^{-1}$ at 2 K, indicating the presence of an antiferromagnetic coupling between the Fe(III) atoms, further confirmed by the presence of a shoulder in the χ_m vs *T* plot (Figure 3) at about

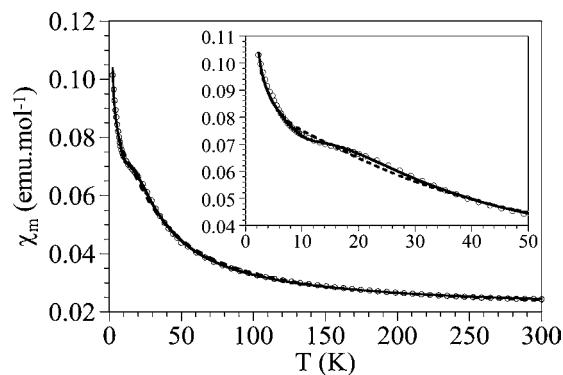


Figure 3. Thermal variation of the molar magnetic susceptibility per Fe(III) dimer for compound **1**. Solid and dashed lines represent the best fit to the $S = 1/2$ and $S = 3/2$ dimer models, respectively. Inset shows the low temperature region.

15 K with a Curie tail at lower temperatures. This antiferromagnetic coupling agrees with the observed behavior in all the similar dithiolato-containing Fe(III) dimers magnetically characterized so far (Table 3).

Interestingly, although at a first sight almost one-half of these Fe(III) dimers with dithiolato ligands contain low spin Fe(III) ions (with a ground spin state $S = 1/2$), a close inspection of the methods used to determine this spin ground state shows that they are not very reliable since most of them are based on electron paramagnetic resonance (EPR) spectra or room temperature magnetic measurements or the data were not fit with any expression. In fact, as can be seen in Table 3, the initial assignment of $S = 1/2$ for compound BMNTFE was later revised by Almeida et al. with more precise measurements in the temperature range 10–300 K that show a $S = 3/2$ spin state. Thus, if we remove these less reliable examples, there are very few Fe dimers with an $S = 1/2$ ground spin state (Table 3). Albeit, we have tried both, the $S = 1/2$ and the $S = 3/2$ dimer models to fit the experimental data of compound **1**.⁵⁸ Although the $S = 1/2$ model gives a slightly better fit, both models

Table 3. Magnetic Properties of All the Characterized Dimeric [Fe(dithiolato)₂]₂ Complexes

CCDC	S	g	J (cm ⁻¹)	Fe–S _{ax} (Å)	Fe–S _{ax} –Fe (deg)	ref.
BMNTE	1/2		<0	2.46		68
	3/2	2.052	–137			77
CEYBOX	1/2 ^a	2.159		2.46		69
	1/2 ^a	2.563				
	3/2 ^a	1.890				
	3/2 ^a	1.952				
DOMVOQ	1/2 ^b	2.263		2.513		70
FINSAW01	1/2 ^b	2.229	<0	2.477		71
HETSEF	3/2	2.099	–179	2.493	80.59	72
MOFYEL	1/2		<0	2.439		73
OLABOS	1/2	1.98	–199	2.476	82.65	38
			–57 inter			
POLHII	3/2	1.81	–192	2.473	81.72	37
TALLUO	3/2	2.0	–228	2.424	81.29	74
		fixed			85.21	
XABSUQ	1/2		<0	2.473		75
YEVBEQ	3/2	1.88	–164	2.501	85.31	76
ZAXJEN	1/2	2.21	–310	2.487	82.05	36
VAGJIX	3/2	2.1	–68	2.72	82.97	62
1	1/2	2.21	–23	2.488	82.04	this work

^aFrom EPR and room temperature magnetic moments measured in solution of CH₂Cl₂ (1.87 μ_B), CH₃CN (2.22 μ_B), DMF (3.66 μ_B), and DMSO (3.78 μ_B). ^bFrom the room temperature magnetic moment.

provide a reasonable good agreement (Figure 3). Nevertheless, the g value obtained for the S = 3/2 dimer model is unrealistic (g = 1.3, dashed line in Figure 3) and, therefore, we conclude that compound **1** presents a low spin S = 1/2 Fe(III) antiferromagnetically coupled dimer with g = 2.21, J = –23 cm⁻¹ and about 4% of paramagnetic Fe(III) monomeric impurity, responsible for the Curie tail observed at very low temperatures in the χ_m plot (solid line in Figure 3).

The isothermal magnetization at 2 K (Supporting Information, Figure S1) shows, as expected, a paramagnetic-like behavior with a weak signal that saturates at about 0.25 μ_B and that can be well reproduced with about 4% of monomeric paramagnetic Fe(III) impurity (solid line in Supporting Information, Figure S1), in agreement with the results of the fit of thermal variation of the magnetic susceptibility.

Electrical Properties. The unusual structural features as well as the presence of sulfur containing ligands⁵⁹ prompted us to study the electrical properties of this compound. Two and four probe direct current (DC) electrical conductivity measurements carried out at electrical voltages in the range –10 to 10 V, at 300 K, on ten different crystals of **1** showed conductivity values of about 10⁻⁵–10⁻⁶ S·cm⁻¹ (Supporting Information, Figure S2) During the first cooling scan (orange line in Figure 4) between about 310 and 280 K the resistivity shows a metallic-like drop of a factor of 2, from about 10⁻⁶ to about 5 × 10⁻⁵ S·cm⁻¹ (this drop can be as high as 2 orders of magnitude and take place at temperatures as low as 240 K, depending on the crystal, Supporting Information, Figures S3–S5). Below about 280 K the resistivity shows again a semiconducting behavior with an activation energy of about 300 meV, and below about 150 K the resistivity becomes too high to be measured by our equipment (above 5 × 10¹¹ Ω). Interestingly, when the sample is heated (red line in Figure 4), the transition

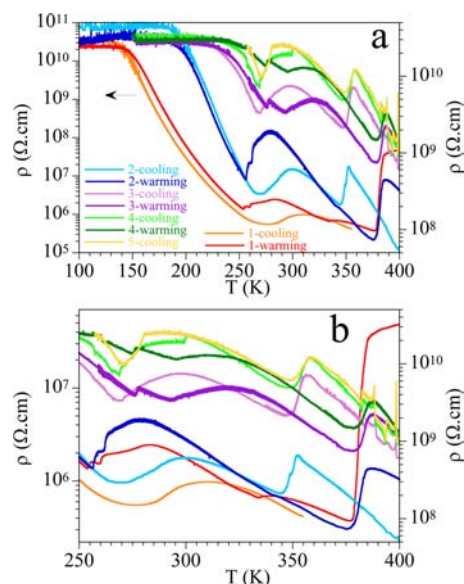


Figure 4. (a) Thermal variation of the resistivity (log scale) of compound **1** in four consecutive cooling and warming cycles (the first cycle is represented in the left scale). (b) A closeup view of the high temperature region.

back to the high resistivity region takes place at a lower temperature (between 250 and 280 K, although in other crystals the transition may take place at temperatures as high as 310 K). On further heating the sample, the resistivity shows a second transition that appears as an abrupt increase of about 2 orders of magnitude at about 380 K. After reaching 400 K, in the cooling scan (light blue line in Figure 4) this abrupt transition is now observed at about 350 K, that is, with a hysteresis of about 30 K (Figure 4b). On further cooling, the transition around room temperature is again observed at approximately the same temperature. The successive warming and cooling cycles show essentially the same behavior as the first ones although the resistivity is higher after each cycle, probably because of the occurrence of microbreaks in the crystal that are clearly observed under the microscope in the crystals after the measurements (Supporting Information, Figure S6). Besides the increase in the resistivity, the third and fourth scans show a “normal” hysteresis in the transition around room temperature and present small steps in the temperature range 250–300 K, also observed in other crystals (Supporting Information, Figure S3–S5). These steps, together with the variability in the transition temperature and its dependence with the cooling and warming rates, suggest that in the 300–250 K range there are two different states coexisting with very weak energy differences.

Although there are several [M(dithiolato)₂]ⁿ⁻ complexes which are semiconductors, metallic conductors, and even superconductors,⁶⁰ there are only four known examples of conducting compounds containing the dimerized [Fe(dithiolato)₂]₂ unit. In two of these four examples the conductivity is due to the presence of the donor bis(ethylenedithia)tetrathiafulvalene (BEDT-TTF = ET),^{61,62} a radical cation of the tetrathiafulvalene (TTF) family. In the two remaining known examples the conductivity is attributed to the presence of a partial oxidation of the [Fe(dithiolato)₂]₂ units together with the presence of short intermolecular S⋯S contacts allowing the delocalization of the electrons.^{63,64}

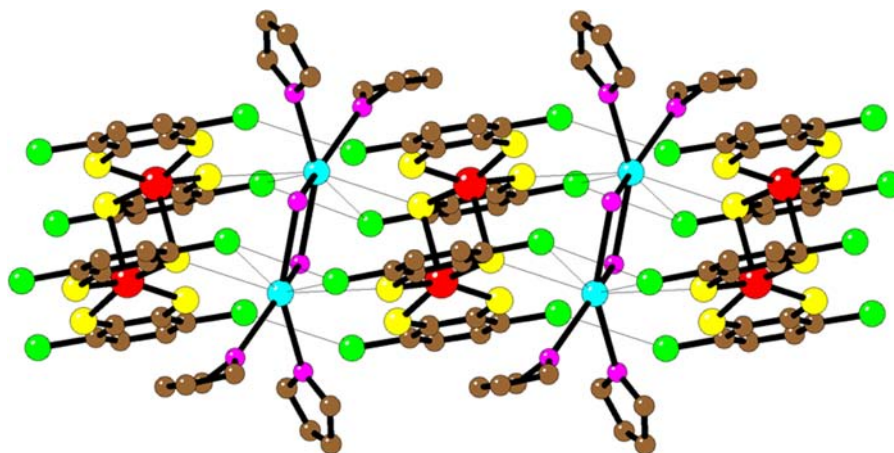


Figure 5. Chain structure of compound **1** showing the shortest anion–cation $K\cdots S$ and $K\cdots Cl$ contacts and interanion $Cl\cdots Cl$ halogen bridges. Color code: C, brown; O, pink; S, yellow; Fe, red; Cl, green; and K, cyan.

In the case of complex **1** a careful analysis of the structure shows that there are only two possible delocalization paths: (i) the anion–cation connection via the $S_{\text{dithiolato}}\cdots K^+$ bonds (with $S-K$ bond distances of about 3.2–3.3 Å) and a $Cl-K$ bond (with a $Cl-K$ bond distance of 3.35 Å) (Figure 5) and (ii) the $Cl\cdots Cl$ halogen bonds with shortest interdimer $Cl-Cl$ distances of 3.40 and 3.46 Å (Figure 5). Since the K^+ ion is not able to delocalize electrons, we can assume that the electron delocalization must take place via the $Cl\cdots Cl$ halogen bonds (option ii). Although, as far as we know, electrical conductivity has never been observed through this kind of $Cl\cdots Cl$ bridges, there are some examples of Cl bridges connecting two metal atoms with high electrical conductivities.^{65,66} Note also that the conductivity values are very low, as expected for such a $Cl\cdots Cl$ bridge. Assuming this pathway for the electronic delocalization we can deduce that the two transitions observed in the thermal variation of the resistivity of compound **1** might be associated to slight changes in the $[Fe(\text{dithiolato})_2]_2$ anions. These changes would modify the $Cl\cdots Cl$ interactions (distance and angles) leading to a change in the orbital overlap and, hence, in the electrical resistivity. Note that a small rotation of the $[Fe(\text{dithiolato})_2]_2$ anions is expected to yield a big change in the orbital overlap and, thus, in the electrical conductivity. Since these changes do not imply any modification inside the $[Fe(\text{dithiolato})_2]_2$ dimer, the magnetic properties are not expected to change, as observed experimentally. The energy difference between the different structures is expected to be very low, in agreement with the observed coexistence of both phases in a large temperature range.

Differential Scanning Calorimetric Studies. Since a single crystal detailed structural analysis of the transitions observed in the resistivity measurements has not been feasible because of the low crystallinity of the available single crystals, we have performed DSC studies to confirm the presence of the transitions and their anomalous hysteretic behaviors (Figure 6). In general these measurements confirm the resistivity data. Thus, in the first cooling scan the sample shows a first endothermic transition (I) at about 300 K with a smooth exothermic one (II) at about 260 K (Figure 6) (very close to the values observed in the resistivity measurements, Figure 4). The first warming scan shows a very tiny exothermic transition (III) at about 260 K (corresponding to the smooth steps observed in the resistivity measurements at this temperature) followed by an abrupt endothermic transition (I) at about 300

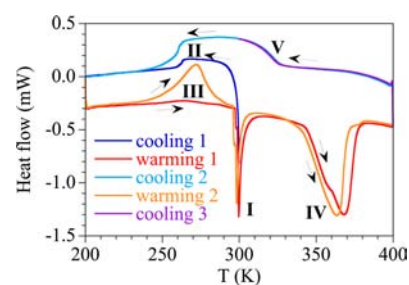


Figure 6. DSC of a polycrystalline sample of compound **1** showing different cooling and warming cycles in the temperature range 400–200 K.

K. On further heating the sample, a deep and large endothermic peak (IV) can be observed in the temperature range 350–380 K (Figure 6), corresponding to the transition observed at 370–380 K in the resistivity measurements (Figure 4). The second cooling scan shows a very large exothermic peak in the temperature range 320–270 K (V–II), corresponding to the hysteresis observed in the second and successive thermal cycles of the resistivity measurements (blue lines in Figure 4) and confirming the existence of a large transition taking place between about 260 and about 320 K. The second heating scan now shows an intense exothermic peak (III) at about 270 K followed by the abrupt one (I) at about 300 K and the large one (IV) at about 350–370 K. In summary, the DSC measurements show the presence of two different transitions with hysteretic behavior and with a temperature range between about 260 and 320 K where both states coexist, as already observed in the resistivity measurements.

CONCLUSIONS

$[K_2(\mu\text{-H}_2\text{O})_2(\text{THF})_4]_n[Fe_2(S_2C_6H_2Cl_2)_4]_n$ is the first example of an iron dithiolene derivative that crystallizes as a 1D coordination polymer. The magnetic properties of **1** show pairwise Fe–Fe antiferromagnetic interactions that can be well reproduced with a coupling constant of -23 cm^{-1} . Albeit, the most interesting aspect of **1** is the fact that this compound is an electrical semiconductor (probably because of the presence of interdimer $Cl\cdots Cl$ interactions) and presents two transitions at high temperatures: one at about 260–320 K with a large hysteresis of more than 50 K around room temperature and a second one at about 350–370 K with a hysteresis of more than

20 K. Interestingly, as far as we know, compound **1** is the first coordination polymer containing an “s” group metal as a bridging building block showing electrical conductivity. Compound **1** represents, on the one hand, the first example of a coordination polymer showing two electrical transitions,⁴⁷ and on the other hand, the second example of a coordination polymer with electrical bistability. As far as we know there is only one very recent example of a coordination polymer showing such bistability (arising from a spin crossover transition).⁶⁷ Compound **1** opens the door to the synthesis and study of novel related coordination polymers presenting coexistence of magnetic and electrical properties. Attempts to prepare these types of compounds by simply changing the coordinating groups in the dithiolato-derivative ligand, the coordinating solvent, or using other magnetic transition metal ions and “s” block cations are under study.

■ ASSOCIATED CONTENT

■ Supporting Information

Crystallographic data in CIF format. Experimental procedures and additional figures. CCDC reference number for compound **1**: 888484. This material is available free of charge via the Internet at <http://pubs.acs.org>.

■ AUTHOR INFORMATION

■ Corresponding Author

*E-mail: esther.delgado@uam.es (E.D.), felix.zamora@uam.es (F.Z.).

■ Notes

The authors declare no competing financial interest.

■ ACKNOWLEDGMENTS

Financial support from Spain's MICINN (CTQ2011-26507 and MAT2010-20843-C02-01), Generalitat Valenciana (Project Prometeo 2009/95) and Factoria de Crystalización (CON-SOLIDER-INGENIO 2010) is gratefully acknowledged.

■ REFERENCES

- (1) Robertson, N.; Cronin, L. *Coord. Chem. Rev.* **2002**, *227*, 93.
- (2) *Dithiolene Chemistry: Synthesis, Properties, and Applications*; Karlin, K. D., Tiefel, E. I., Eds.; John Wiley and Sons: New York, 2004; Vol. 52.
- (3) Muller-Westerhoff, U. T.; Vance, B. In *Comprehensive Coordination Chemistry*; Pergamon Press: Oxford, U.K., 1987; Vol. 2.
- (4) Clemenson, P. I. *Coord. Chem. Rev.* **1990**, *106*, 171.
- (5) Belo, D.; Almeida, M. *Coord. Chem. Rev.* **2010**, *254*, 1479.
- (6) Ezzaher, S.; Gogoll, A.; Bruhn, C.; Ott, S. *Chem. Commun.* **2010**, *46*, 5775.
- (7) Alcácer, L.; Novais, H. In *Extended Linear Chain Compounds*; Miller, E. J. S., Ed.; Plenum Press: New York, 1983; p 319.
- (8) Cassoux, P.; Valade, L.; Kobayashi, H.; Kobayashi, A.; Clark, R. A.; Underhill, A. E. *Coord. Chem. Rev.* **1991**, *110*, 115.
- (9) Alcácer, L.; Novais, H.; Pedroso, F.; Flandrois, S.; Coulon, C.; Chasseau, D.; Gaultier, J. *Solid State Commun.* **1980**, *35*, 945.
- (10) Alcácer, L.; Maki, A. H. *J. Phys. Chem.* **1974**, *78*, 215.
- (11) Alcácer, L.; Maki, A. H. *J. Phys. Chem.* **1976**, *80*, 1912.
- (12) Belo, D.; Figueira, M. J.; Santos, I. C.; Gama, V.; Pereira, L. C.; Henriques, R. T.; Almeida, M. *Polyhedron* **2005**, *24*, 2035.
- (13) Nunes, J. P. M.; Figueira, M. J.; Belo, D.; Santos, I. C.; Ribeiro, B.; Lopes, E. B.; Henriques, R. T.; Vidal-Gancedo, J.; Veciana, J.; Rovira, C.; Almeida, M. *Chem.—Eur. J.* **2007**, *13*, 9841.
- (14) Sproules, S.; Wiegardt, K. *Coord. Chem. Rev.* **2010**, *254*, 1358.
- (15) Rabaca, S.; Almeida, M. *Coord. Chem. Rev.* **2010**, *254*, 1493.
- (16) Schwartz, L.; Singh, P. S.; Eriksson, L.; Lomoth, R.; Ott, S. C. R. *Chim.* **2008**, *11*, 875.
- (17) Schwartz, L.; Eriksson, L.; Lomoth, R.; Teixidor, F.; Vinas, C.; Ott, S. *Dalton Trans.* **2008**, 2379.
- (18) Si, Y.; Hu, M.; Chen, C. C. R. *Chim.* **2008**, *11*, 9328.
- (19) Gloaguen, F.; Lawrence, J. D.; Schmidt, M.; Wilson, S. R.; Rauchfuss, T. B. *J. Am. Chem. Soc.* **2001**, *123*, 12518.
- (20) Gloaguen, F.; Lawrence, J. D.; Rauchfuss, T. B. *J. Am. Chem. Soc.* **2001**, *123*, 9476.
- (21) Zhao, X.; Georgakaki, I. P.; Miller, M. L.; Mejia-Rodriguez, R.; Chiang, C. Y.; Darensbourg, M. Y. *Inorg. Chem.* **2002**, *41*, 3917.
- (22) Gloaguen, F.; Lawrence, J. D.; Rauchfuss, T. B.; Benard, M.; Rohmer, M. M. *Inorg. Chem.* **2002**, *41*, 6573.
- (23) Song, L. C.; Yang, Z. Y.; Hua, Y. J.; Wang, H. T.; Liu, Y.; Hu, Q. M. *Organometallics* **2007**, *26*, 2106.
- (24) Rauchfuss, T. B.; Contakes, S. M.; Hsu, S. C. N.; Reynolds, M. A.; Wilson, S. R. *J. Am. Chem. Soc.* **2001**, *123*, 6933.
- (25) Streich, D.; Karnahl, M.; Astuti, Y.; Cady, C. W.; Hammarstrom, L.; Lomoth, R.; Ott, S. *Eur. J. Inorg. Chem.* **2011**, 1106.
- (26) Lee, C. M.; Hsieh, C. H.; Dutta, A.; Lee, G. H.; Liaw, W. F. *J. Am. Chem. Soc.* **2003**, *125*, 11492.
- (27) Kitagawa, S.; Noro, S. In *Comprehensive Coordination Chemistry II*; Elsevier: Amsterdam, The Netherlands, 2004; Vol. 7.
- (28) Batten, S. R.; Neville, S. M.; Turner, D. *Coordination Polymers: Design, Analysis and Applications*; RSC Publishing: Cambridge, U.K., 2009; Vol. 7.
- (29) *Purification of Laboratory Chemicals*, 4th ed.; Perrin, D. D., Armarego, W. L. F., Eds.; Pergamon Press Ltd.: Oxford, U.K., 2002.
- (30) Bain, G. A.; Berry, J. F. *J. Chem. Educ.* **2008**, *85*, 532.
- (31) Farrugia, L. J. *J. Appl. Crystallogr.* **1999**, *32*, 837.
- (32) Sheldrick, G. M. *Acta Crystallogr.* **2008**, *A64*, 112.
- (33) Gao, X. K.; Dou, H. M.; Li, D. C.; Dong, F. Y.; Wang, D. Q. *J. Mol. Struct.* **2005**, *733*, 181.
- (34) Dong, F. Y.; Dou, J. M.; Li, D. C.; Gao, X. K.; Wang, D. Q. *J. Inorg. Organomet. Polym. Mater.* **2005**, *15*, 231.
- (35) Jeannin, O.; Clerac, R.; Cauchy, T.; Fourmigue, M. *Inorg. Chem.* **2008**, *47*, 10656.
- (36) Fettouhi, M.; Ouahab, L.; Hagiwara, M.; Codjovi, E.; Kahn, O.; Constantmachado, H.; Varret, F. *Inorg. Chem.* **1995**, *34*, 4152.
- (37) Cerdeira, A. C.; Simao, D.; Santos, I. C.; Machado, A.; Pereira, L. C. J.; Waerenborgh, J. C.; Henriques, R. T.; Almeida, M. *Inorg. Chim. Acta* **2008**, *361*, 3836.
- (38) Alves, H.; Simao, D.; Novais, H.; Santos, I. C.; Gimenez-Saiz, C.; Gama, V.; Waerenborgh, J. C.; Henriques, R. T.; Almeida, M. *Polyhedron* **2003**, *22*, 2481.
- (39) Simao, D.; Ayllon, J. A.; Rabaca, S.; Figueira, M. J.; Santos, I. C.; Henriques, R. T.; Almeida, M. *Cryst. Eng. Commun.* **2006**, *8*, 658.
- (40) Yamaguchi, T.; Masaoka, S.; Sakai, K. *Acta Crystallogr., Sect. E* **2009**, *65*, M77.
- (41) Bondi, A. J. *Phys. Chem.* **1964**, *68*, 441.
- (42) Nyburg, S. C.; Faerman, C. H. *Acta Crystallogr., Sect. B* **1985**, *41*, 274.
- (43) Fourmigue, M.; Batail, P. *Chem. Rev.* **2004**, *104*, 5379.
- (44) Fourmigué, M. *Struct. Bonding (Berlin)* **2008**, *126*, 181.
- (45) Gowda, B. T.; Foro, S.; Shakuntala, K. *Acta Crystallogr., Sect. E* **2011**, *67*, M1015.
- (46) Gowda, B. T.; Foro, S.; Shakuntala, K. *Acta Crystallogr., Sect. E* **2011**, *67*, M914.
- (47) Bergougnant, R. D.; Robin, A. Y.; Fromm, K. M. *Cryst. Growth. Des.* **2005**, *5*, 1691.
- (48) Chadwick, S.; Englich, U.; Ruhlandt-Senge, K. *Organometallics* **1997**, *16*, 5792.
- (49) Hu, J. X.; Barbour, L. J.; Gokel, G. W. *Chem. Commun.* **2002**, 1808.
- (50) Molcanov, K.; Kojic-Prodic, B.; Babic, D.; Zilic, D.; Rakvin, B. *Cryst. Eng. Commun.* **2011**, *13*, 5170.
- (51) Osterloh, F.; Segal, B. M.; Achim, C.; Holm, R. H. *Inorg. Chem.* **2000**, *39*, 980.
- (52) Paluch, K. J.; Tajber, L.; McCabe, T.; O'Brien, J. E.; Corrigan, O. I.; Healy, A. M. *Eur. J. Pharm. Sci.* **2011**, *42*, 220.

- (53) Rosokha, S. V.; Lu, J. J.; Rosokha, T. Y.; Kochi, J. K. *Phys. Chem. Chem. Phys.* **2009**, *11*, 324.
- (54) Sporer, C.; Ratera, I.; Ruiz-Molina, D.; Gancedo, J. V.; Ventosa, N.; Wurst, K.; Jaitner, P.; Rovira, C.; Veciana, J. *Solid State Sci.* **2009**, *11*, 786.
- (55) Sporer, C.; Ratera, I.; Ruiz-Molina, D.; Gancedo, J. V.; Wurst, K.; Jaitner, P.; Rovira, C.; Veciana, J. *J. Phys. Chem. Solids* **2004**, *65*, 753.
- (56) Gowda, B. T.; Babitha, K. S.; Svoboda, I.; Fuess, H. *Acta Crystallogr., Sect. E* **2007**, *63*, M2222.
- (57) Cambridge Crystallographic Data Base, Conquest v1.14, 2012.
- (58) O'Connor, C. J. *Prog. Inorg. Chem.* **1982**, *29*, 203.
- (59) Givaja, G.; Amo-Ochoa, P.; Gómez-García, C. J.; Zamora, F. *Chem. Soc. Rev.* **2012**, *41*, 115.
- (60) Cassoux, P. *Coord. Chem. Rev.* **1999**, *185–6*, 213.
- (61) Fettouhi, M.; Waheed, A.; Golhen, S.; Helou, N.; Ouahab, L.; Molinie, P. *Synth. Met.* **1999**, *102*, 1764.
- (62) Deplano, P.; Leoni, L.; Mercuri, M. L.; Schlueter, J. A.; Geiser, U.; Wang, H. H.; Kini, A. M.; Manson, J. L.; Gomez-Garcia, C. J.; Coronado, E.; Koo, K. J.; Whangbo, M. H. *J. Mater. Chem.* **2002**, *12*, 3570.
- (63) Tanaka, S.; Matsubayashi, G. *J. Chem. Soc., Dalton Trans.* **1992**, 2837.
- (64) Kubel, F.; Valade, L.; Strahle, J.; Cassoux, P. *C. R. Acad. Sci. II* **1982**, *295*, 179.
- (65) Kitagawa, H.; Onodera, N.; Sonoyama, T.; Yamamoto, M.; Fukawa, T.; Mitani, T.; Seto, M.; Maeda, Y. *J. Am. Chem. Soc.* **1999**, *121*, 10068.
- (66) Mitsumi, M.; Murase, T.; Kishida, H.; Yoshinari, T.; Ozawa, Y.; Toriumi, K.; Sonoyama, T.; Kitagawa, H.; Mitani, T. *J. Am. Chem. Soc.* **2001**, *123*, 11179.
- (67) Rotaru, A.; Gural'skiy, I. A.; Molnar, G.; Salmon, L.; Demont, P.; Bousseksou, A. *Chem. Commun.* **2012**, *48*, 4163.
- (68) Hamilton, W. C.; Bernal, I. *Inorg. Chem.* **1967**, *6*, 2003.
- (69) Kanatzidis, M. G.; Coucouvanis, D. *Inorg. Chem.* **1984**, *23*, 403.
- (70) Sawyer, D. T.; Srivatsa, G. S.; Bodini, M. E.; Schaefer, W. P.; Wing, R. M. *J. Am. Chem. Soc.* **1986**, *108*, 936.
- (71) Kang, B. S.; Weng, L. H.; Wu, D. X.; Wang, F.; Guo, Z.; Huang, L. R.; Huang, Z. Y.; Liu, H. Q. *Inorg. Chem.* **1988**, *27*, 1128.
- (72) Rodrigues, J. V.; Santos, I. C.; Gama, V.; Henriques, R. T.; Waerenborgh, J. C.; Duarte, M. T.; Almeida, M. *J. Chem. Soc., Dalton Trans.* **1994**, 2655.
- (73) Ren, X. M.; Wu, P. H.; Zhang, W. W.; Meng, Q. J.; Chen, X. Y. *Trans. Met. Chem.* **2002**, *27*, 394.
- (74) Ray, K.; Bill, E.; Weyhermuller, T.; Wieghardt, K. *J. Am. Chem. Soc.* **2005**, *127*, 5641.
- (75) Coucouvanis, D.; Paital, A. R.; Zhang, Q. W.; Lehnert, N.; Ahlrichs, R.; Fink, K.; Fenske, D.; Powell, A. K.; Lan, Y. H. *Inorg. Chem.* **2009**, *48*, 8830.
- (76) Awaga, K.; Okuno, T.; Maruyama, Y.; Kobayashi, A.; Kobayashi, H.; Schenk, S.; Underhill, A. E. *Inorg. Chem.* **1994**, *33*, 5598.
- (77) Gama, V.; Henriques, R. T.; Bonfait, G.; Pereira, L. C.; Waerenborgh, J. C.; Santos, I. C.; Duarte, M. T.; Cabral, J. M. P.; Almeida, M. *Inorg. Chem.* **1992**, *31*, 2598.